

# Antenna-Coupled Niobium Bolometers for Terahertz Spectroscopy

Daniel F. Santavicca, Matthew O. Reese, Alan B. True, Charles A. Schmuttenmaer, and Daniel E. Prober, *Member, IEEE*

**Abstract**—We report characterizations of antenna-coupled hot electron bolometers designed for laboratory-based terahertz spectroscopy. These direct detectors combine sub-nanosecond response, high sensitivity, and the ability to operate below saturation when viewing a room temperature background. The optimum small-signal responsivity is  $4.4 \times 10^4$  V/W, measured at a bath temperature  $T_b \approx 0.9T_c$ . The corresponding saturation power is 7 nW. The saturation power increases and the small-signal responsivity decreases as the bath temperature is lowered. The measured noise equivalent power is  $2.0 \times 10^{-14}$  W/(Hz)<sup>1/2</sup>, near the predicted thermal fluctuation limit. The noise is white from approximately 100 Hz to 100 MHz.

**Index Terms**—Bolometers, submillimeter wave detectors, superconducting devices.

## I. INTRODUCTION

THE development of ultra-sensitive superconducting detectors has recently led to predictions of achievable single photon sensitivity in the far-infrared [1], [2] with important applications in radioastronomy [3], [4]. These detectors are designed for satellite-based observation, as they would be driven into saturation by a room temperature background. For laboratory-based terahertz (THz) spectroscopy, the two commonly used detector types are the large-area bolometer [5] and the photoconducting antenna [6]. The most sensitive silicon bolometers are slow ( $\sim$ ms) and require bath temperatures below 1 K for optimal sensitivity. Photoconducting antennas operate at room temperature and are extremely fast, but for maximum sensitivity they require a synchronous pulsed detection scheme that is impractical for some applications [7]. Neither detector is practical for measurements of the evolution of dynamic systems on nanosecond to millisecond timescales, which is too fast for typical commercial bolometers and too long for an optical delay line.

We have developed a superconducting hot electron direct detector that has a sub-nanosecond response, operates at a convenient bath temperature of 4.2 K, and is designed to optimize the tradeoff between sensitivity and saturation when viewing a room temperature source. This combination of properties makes the device uniquely well suited for a variety of applications in

Manuscript received August 29, 2006. This work was supported by NSF-CHE-0616875, NSF-DMR-0407082, NSF-AST-0138318, and a NASA GSRP fellowship (to MOR).

D. F. Santavicca, M. O. Reese, and D. E. Prober are with the Department of Applied Physics, Yale University, New Haven, CT 06511 USA (e-mail: daniel.santavicca@yale.edu).

A. B. True and C. A. Schmuttenmaer are with the Department of Chemistry, Yale University, New Haven, CT 06511 USA.

Digital Object Identifier 10.1109/TASC.2007.898191

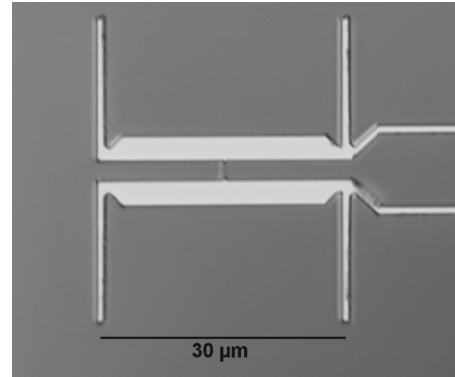


Fig. 1. Optical image of a niobium hot electron bolometer with double-dipole antenna on a silicon substrate.

laboratory THz spectroscopy, such as studies of transient photoconductivity in molecular and nanocrystal ensembles [8] and the decay of highly excited molecular species similar to those found in protostellar molecular clouds [3].

Previous work on an antenna-coupled niobium microbridge suspended over a vacuum gap measured a noise equivalent power (NEP) of  $1.4 \times 10^{-14}$  W/(Hz)<sup>1/2</sup> at a bath temperature of 4.2 K, but with a response that is significantly slower than the device we present [9]. (The response exhibited a roll-off above 50 kHz that was attributed to the SQUID readout.) Recently, a large-area niobium bolometer has been commercially developed by QMC Instruments. It has a fast response, similar to our device, but much lower sensitivity, with a quoted optical NEP of  $2 \times 10^{-11}$  W/(Hz)<sup>1/2</sup> [10].

Antenna coupling enables a significantly smaller, more sensitive detector element. The antenna couples to photons of a single mode and spatial polarization, collecting much less background power ( $\sim$ nW) than large-area bolometers, which typically use a multi-mode Winston cone to couple to the device. The geometry of our device is seen in Fig. 1. The planar antenna structure consists of two half-wave dipoles and is designed for a detection bandwidth of 0.8–1.6 THz in a silicon environment [11]. Larger bandwidth antenna designs are possible [12]. The antenna is composed of 12 nm of niobium covered by 200 nm of aluminum with a sheet resistance of less than 0.1  $\Omega$ /square. A choke structure prevents loss of the THz signal to the biasing and readout ports but allows dc-GHz input and output with near unity efficiency.

The superconducting niobium microbridge, oriented at the center of the antenna, serves as both the absorber and thermometer. It is approximately 2.5  $\mu$ m long, 1  $\mu$ m wide, and

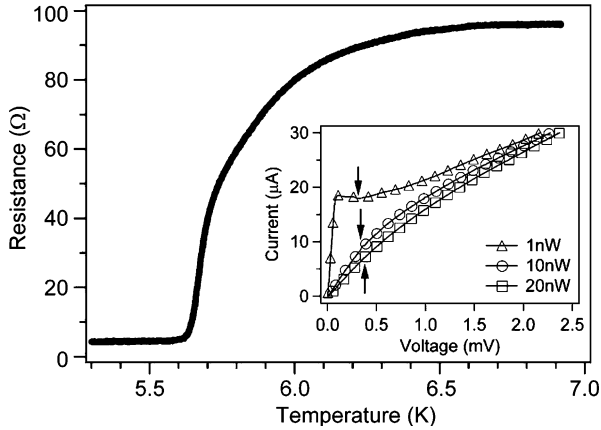


Fig. 2. Resistance versus temperature curve measured with  $I_{dc} = 1 \mu\text{A}$ . Inset: Current versus voltage curves at  $T_b = 5.2 \text{ K}$  taken with different applied microwave powers. Arrows indicate the optimum bias point for detection.

12 nm thick. The device was fabricated using a process originally developed for smaller microbridges which has been described elsewhere [13]. The response time of the device is set by the electron-phonon time, measured to be 0.7 ns. This is consistent with previous measurements of the electron-phonon time in thin niobium films [14], [15].

Typical dc characterizations are presented in Fig. 2. The normal state resistance is 96  $\Omega$ . The critical temperature,  $T_c$ , measured with  $I_{dc} = 1 \mu\text{A}$  is approximately 5.8 K. The current-voltage (IV) curves were measured with a 20  $\Omega$  dc load line, the same dc biasing condition used in detection. The optimum bias point for detection is indicated on each IV curve with an arrow.

We have measured the device response to a broadband, pulsed THz source; to a thermal source (hot-cold load); and to a time-varying microwave signal. Two devices were studied, with similar dc properties. One was studied at microwave frequencies and the other at THz frequencies. The microwave characterization allowed us to test over a broader range of conditions than is convenient in the THz test system. We measured the responsivity as a function of dc voltage and signal power at different bath temperatures. In the THz test system, the device was mounted on a hyper-hemispherical silicon lens in an optical access cryostat. Measurements of the response to a known thermal source enabled us to determine the optical coupling efficiency. The noise performance was measured in both systems.

## II. MICROWAVE CHARACTERIZATION

The microwave characterizations were performed with the sample mounted in a vacuum can in a pumped  $^4\text{He}$  cryostat. Negligible infrared radiation reached the device. The sample temperature could be adjusted above the bath temperature with a simple heater block. This experimental setup is similar to one described previously [15], except electrical coupling to the device was achieved with wirebonds rather than a flip-chip technique. An  $\approx 1 \text{ GHz}$  input signal was amplitude modulated at 80 MHz, and the device response was measured at the modulation frequency with a low noise cryogenic amplifier coupled to a spectrum analyser.

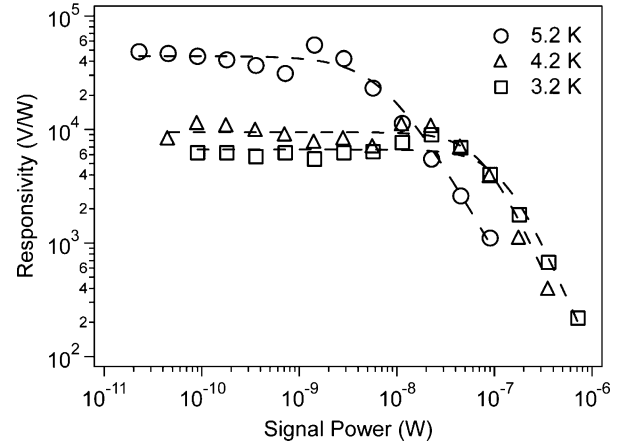


Fig. 3. Optimum responsivity as a function of signal power at different bath temperatures. Dashed lines are a fit to (1).

We measured the responsivity,  $R$ , as a function of dc voltage, bath temperature, and signal power. The responsivity is defined as the change in voltage measured at the input of the 50  $\Omega$  amplifier divided by the absorbed signal power, in V/W. The responsivity at the optimum bias voltage as a function of the modulated signal power is presented in Fig. 3 for three different bath temperatures. The largest responsivity is obtained for bath temperatures near  $T_c$ . This is in contrast to similar devices employed as heterodyne mixers, where the largest response is obtained at low temperature ( $T_b \leq T_c/2$ ) as a result of the use of a local oscillator [15]. Operating near  $T_c$  has the additional benefit of excellent biasing stability due to the rounded features and non-hysteretic quality of the IV curve.

The saturation power is defined as the absorbed power at which the responsivity decreases from its small signal value ( $P \ll P_{sat}$ ) by a factor of two. The optimum responsivity at a given  $T_b$  approximately follows the empirical relation

$$R(P) = \frac{R(0)}{1 + \left(\frac{P}{P_{sat}}\right)^\alpha} \quad (1)$$

where  $\alpha = 1.5$  at  $T_b = 5.2 \text{ K}$  and  $\alpha = 2$  at  $T_b = 4.2 \text{ K}$  and 3.2 K. The saturation powers at 5.2 K, 4.2 K, and 3.2 K are, respectively, 7 nW, 79 nW, and 126 nW. The tradeoff between responsivity and saturation can be optimized for a particular application by an appropriate choice of bath temperature.

## III. THZ CHARACTERIZATION

Devices were fabricated on a high resistivity silicon substrate for quasi-optical coupling. We lithographically patterned a silicon wafer with alignment marks on each side using a back-side optical alignment technique. The substrate with the device was aligned on one side of this wafer and attached with UV-curable adhesive, and a 6 mm diameter hyperhemispherical silicon lens was aligned and attached on the opposite side. The detector was at the silicon-air interface. We estimate that the alignment accuracy is within  $\pm 10 \mu\text{m}$ .

The antenna response at a silicon-air interface was simulated in Microwave Office. The results show a response

peak at 1.8 THz with an integrated bandwidth of approximately 1.0 THz. Experimental antenna characterizations are in progress and will be reported in a future publication.

The device response over the full antenna bandwidth was measured by switching between hot and cold thermal sources at 315 Hz. The hot source (295 K) was the surface of the chopping wheel coated in a mixture of Stycast 2850FT and 1 mm silicon carbide grains [16]. The cold source (77 K) was an 8 mm thick piece of Eccosorb foam dipped in liquid nitrogen. A Zitex G110 membrane was used as an infrared filter on the heat shield window [17]. The available power from each source was found by integrating the one-dimensional Planck thermal spectrum over the antenna bandwidth [18]. Assuming the same responsivity as measured in the microwave characterization [15], [19], we find an optical coupling efficiency, defined as the ratio of power absorbed in the device to power incident on the cryostat window, of  $\eta = 0.15$ .

We also measured the response to a broadband, pulsed THz source. This source is based on a photoconductive switch driven by a Ti:Sapphire laser oscillator and has been described previously [8]. The switch consists of a semi-insulating GaAs 100 wafer with a pair of electrodes separated by 30  $\mu\text{m}$  that have a 10 V dc bias applied, and roughly 200 mW are used to drive the switch. The fast response of our detector allowed us to detect directly at the 80 MHz pulse repetition rate. Based on the measured responsivity and optical coupling efficiency, we determined that the THz signal power external to the cryostat is  $\approx 1$  nW. This is consistent with previous work on a similar experimental setup [6].

#### IV. NOISE PERFORMANCE

The measured noise has contributions from photon shot noise, from intrinsic device noise, and from amplifier noise. These noise sources are uncorrelated and the noise amplitudes add in quadrature. Within the response bandwidth, intrinsic device noise is predominately due to thermal fluctuations, although at low frequencies  $1/f$  noise may become significant. It is customary to express the sensitivity as a noise equivalent power (NEP), defined as the input power that can be resolved with a signal to noise ratio of one in a one hertz output bandwidth, in  $\text{W}/(\text{Hz})^{1/2}$ .

The NEP due to photon shot noise in the Rayleigh-Jeans limit is given by [5]

$$\text{NEP}_{\text{photon}} = \eta kT \sqrt{2\Delta f} \quad (2)$$

where  $\eta$  is the optical coupling efficiency and  $\Delta f$  is the detection bandwidth. For  $\eta = 0.15$ ,  $T = 295$  K, and  $\Delta f = 1.0$  THz, we get  $\text{NEP}_{\text{photon}} = 8.6 \times 10^{-16} \text{ W}/(\text{Hz})^{1/2}$ . The amplifier noise, measured separately, is approximately  $1 \times 10^{-14} \text{ W}/(\text{Hz})^{1/2}$  in both test systems. The thermal fluctuation noise is given by [5]

$$\text{NEP}_{\text{th}} = \sqrt{4kT^2G} \quad (3)$$

where  $T$  is the average bridge temperature and  $G$  is the thermal conductance between the electron system in the bridge and the bridge/substrate phonons.

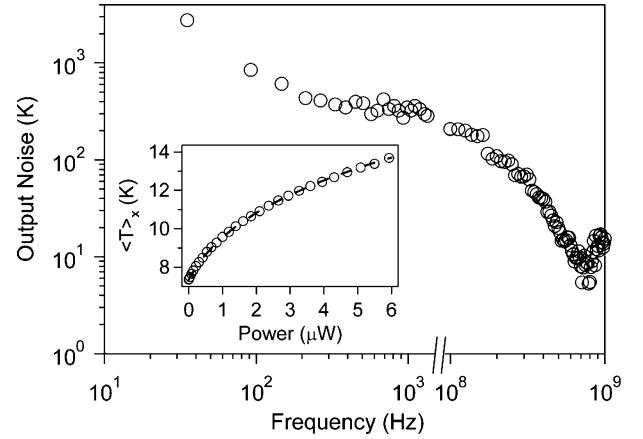


Fig. 4. Output noise as a function of frequency (amplifier contribution has been subtracted). Note the discontinuity in the frequency axis. Inset: Average electron temperature as a function of applied dc power to determine the thermal conductance  $G$ , as described in the text. Dashed line is a fit to (4).

We determined  $G$  via Johnson noise thermometry at 1 GHz [15]. The device was heated above  $T_c$ , and the average bridge temperature  $T = P_N/(kB)$ , where  $P_N$  is the noise power coupled to a matched load and  $B$  is the measurement bandwidth, was measured as a function of applied dc power  $P_{dc}$ . The data were fit to the experimentally established relation

$$P_{dc} = A (T^4 - T_b^4) V \quad (4)$$

where  $V$  is the device volume, to get  $A = 8.2 \times 10^9 \text{ WK}^{-4}\text{m}^{-3}$ , in good agreement with previous work on thin niobium films [14], [15]. This gives a predicted value for the thermal fluctuation noise  $\text{NEP}_{\text{th}} = 1.9 \times 10^{-14} \text{ W}/(\text{Hz})^{1/2}$ .

In both test systems, the output noise was measured at  $T_b = 5.2$  K with the device at the optimum bias point. At audio frequencies, we used a homemade bias tee to minimize the noise from the biasing electronics. The ac signal was fed through an audio transformer to a low noise preamp. At higher frequencies, we used a commercial bias tee and a 50  $\Omega$  amplifier.

The electrical NEP referred to the detector was the same in both systems,  $2.2 \times 10^{-14} \text{ W}/(\text{Hz})^{1/2}$ . Removing the measured amplifier contribution, we get  $\text{NEP}_{\text{device}} = 2.0 \times 10^{-14} \text{ W}/(\text{Hz})^{1/2}$ , close to the predicted value of thermal fluctuation noise. The optical NEP referred to the cryostat window is the electrical NEP divided by the optical coupling efficiency, thus  $\text{NEP}_{\text{optical}} = 1.3 \times 10^{-13} \text{ W}/(\text{Hz})^{1/2}$ .

The output noise as a function of frequency is presented in Fig. 4. The amplifier contribution has been measured separately and subtracted. The noise is white from approximately 100 Hz to 100 MHz. Below 100 Hz,  $1/f$  noise becomes significant. We note that the relatively small  $1/f$  contribution is favorable, as it permits measurements with a mechanical chopper to be performed with similar sensitivity to higher frequency measurements. Above 100 MHz, the output noise rolls off with a frequency dependence that is similar to the signal power, as expected [15]. At frequencies well beyond the response bandwidth, the dominant contribution to intrinsic device noise is Johnson noise.

## V. CONCLUSION

We have demonstrated an antenna-coupled niobium hot electron bolometer with a geometry designed to optimize device parameters for applications in THz spectroscopy from room temperature samples. The peak responsivity is obtained for bath temperatures near  $T_c$ , while the largest saturation powers are obtained at lower bath temperatures. The response time is 0.7 ns, set by the electron-phonon time. The measured sensitivity is near the predicted limit of thermal fluctuation noise.

## ACKNOWLEDGMENT

The authors thank L. Frunzio, P. Pütz, B. Reulet, V. Savu, A. Skalare, and A. Young for assistance and helpful discussions.

## REFERENCES

- [1] R. J. Schoelkopf, S. H. Moseley, C. M. Stahle, P. Wahlgren, and P. Delsing, "A concept for a submillimeter-wave single-photon counter," *IEEE Trans. Appl. Supercond.*, vol. 9, no. 2, pp. 2935–2939, 1999.
- [2] B. S. Karasik, A. V. Sergeev, D. Olaya, J. Wei, M. E. Gershenson, J. H. Kawamura, and W. R. McGrath, "A photon counting hot-electron bolometer for space THz spectroscopy," in *Proc. 16th Annual Symp. Space Terahertz Tech.*, 2005, pp. 543–548.
- [3] G. A. Blake, "Microwave and terahertz spectroscopy," in *Encyclopedia of Chemical Physics and Physical Chemistry*, J. H. Moore and N. D. Spencer, Eds. : Institute of Physics Publishing, 2001.
- [4] P. L. Richards, "Bolometric detectors for measurements of the cosmic microwave background," *J. Supercond: Incorp. Novel Mag.*, vol. 17, no. 5, pp. 545–550, 2004.
- [5] P. L. Richards, "Bolometers for infrared and millimeter waves," *J. Appl. Phys.*, vol. 76, no. 1, pp. 1–24, 1994.
- [6] M. van Exter and D. R. Grischkowsky, "Characterization of an optoelectronic terahertz beam system," *IEEE Trans. Microwave Theory Tech.*, vol. 38, no. 11, pp. 1684–1691, 1990.
- [7] P. Y. Han, M. Tani, M. Usami, S. Kono, R. Kersting, and X.-C. Zhang, "A direct comparison between terahertz time-domain spectroscopy and far-infrared Fourier transform spectroscopy," *J. Appl. Phys.*, vol. 89, no. 4, pp. 2357–2359, 2001.
- [8] C. A. Schmuttenmaer, "Exploring dynamics in the far-infrared with terahertz spectroscopy," *Chem. Rev.*, vol. 104, pp. 1759–1776, 2004.
- [9] A. Luukanen and J. P. Pekola, "A superconducting antenna-coupled hot-spot microbolometer," *Appl. Phys. Lett.*, vol. 82, no. 22, pp. 3970–3972, 2003.
- [10] [Online]. Available: <http://www.terahertz.co.uk/QMCI/qmc.html>
- [11] A. Skalare, T. de Graauw, and H. van de Stadt, "A planar dipole array antenna with an elliptical lens," *Microwave and Optical Tech. Lett.*, vol. 4, no. 1, pp. 9–12, 2001.
- [12] G. M. Rebeiz, "Millimeter-wave and terahertz integrated circuit antennas," *Proc. IEEE*, vol. 80, no. 11, pp. 1748–1770, 1992.
- [13] M. O. Reese, D. F. Santavicca, L. Frunzio, and D. E. Prober, "Hot electron bolometer development for a submillimeter heterodyne array camera," *IEEE Trans. Appl. Supercond.*, this issue.
- [14] E. M. Gershenson, M. E. Gershenson, G. N. Gol'tsman, A. M. Lyul'kin, A. D. Semenov, and A. V. Sergeev, "Electron-phonon interaction in ultrathin Nb films," *Sov. Phys. JETP*, vol. 70, no. 3, pp. 505–511, 1990.
- [15] P. J. Burke, R. J. Schoelkopf, D. E. Prober, A. Skalare, B. S. Karasik, M. C. Gaidis, W. R. McGrath, B. Bumble, and H. G. LeDuc, "Mixing and noise in diffusion and phonon cooled superconducting hot-electron bolometers," *J. Appl. Phys.*, vol. 85, no. 3, pp. 1644–1653, 1999.
- [16] M. C. Diez, T. O. Klassen, S. Smorenburg, V. Kirschner, and K. J. Wildeman, "Reflectance measurements on sub-millimetre absorbing coatings for HIFI," in *UV, Optical, and IR Space Telescopes and Instruments*, J. B. Brekinridge and P. Jakobsen, Eds. : , 2000, vol. 4013, Proc. SPIE, pp. 129–139.
- [17] D. J. Bendford, M. C. Gaidis, and J. W. Kooi, "Optical properties of Zitex in the infrared to submillimeter," *Appl. Opt.*, vol. 42, no. 25, pp. 5118–5122, 2003.
- [18] A. R. Kerr, "Suggestions for revised definitions of noise quantities, including quantum effects," *IEEE Trans. Microwave Theory Tech.*, vol. 47, no. 3, pp. 325–329, 1999.
- [19] E. M. Gershenson, M. E. Gershenson, G. N. Gol'tsman, A. D. Semyonov, and A. V. Sergeev, "Heating of electrons in superconductor in the resistive state due to electromagnetic radiation," *Solid State Comm.*, vol. 50, no. 3, pp. 207–212, 1984.